

The MAVR high-resolution magnetic analyzer setup

V.A. Maslov^{1,*}, S.M. Lukyanov¹, K. Mendibayev^{1,2},
A.V. Shakhov¹, T. Issatayev^{1,2}, D. Aznabayev¹, T.K. Zholdybayev²,
A.M. Zolotarev¹, I.V. Kolesov¹, and Yu.E. Penionzhkevich¹

¹Joint Institute for Nuclear Research, Dubna, Russia

²Institute of Nuclear Physics, Almaty, Kazakhstan

e-mail: maslov_vova@mail.ru

DOI: 10.63907/ansa.v2i1.75

Received: 16 February 2026

Abstract

This paper presents the MAVR high-resolution magnetic analyzer, operating at the U400 cyclotron and the DRIBs radioactive ion beam facility at the Flerov Laboratory of Nuclear Reactions, Joint Institute for Nuclear Research. The analyzer is designed to study nuclear reactions using stable and radioactive ion beams over a wide energy range, from subthreshold energies to 30 MeV per nucleon. Its key features include a large solid angle of 15 msr, high momentum resolution of approximately 10^{-4} , a focal plane length of 1.9 m, and high charge resolution of approximately $1/60$. The detector system includes a position-sensitive ionization chamber, time-of-flight detectors, and silicon strip detectors, providing reliable identification of reaction products by their mass number A and atomic number Z . The optical properties of the analyzer were studied using the MAVRPC code and confirmed experimentally. The possibility of operating in gas-filled mode for heavy ion studies is also discussed.

1 Introduction

Studies of nuclear reaction mechanisms with beams of rare stable nuclei such as ^{36}S , ^{48}Ca , ^{58}Fe , ^{64}Ni , and ^{136}Xe , as well as with radioactive ion beams over a wide energy range from sub-barrier energies up to 30 MeV/nucleon are of considerable interest for the production of new exotic nuclei, the investigation of their unusual structure and its influence on reaction mechanisms, and for the development of theoretical models related to problems of nuclear astrophysics.

The high-resolution magnetic analyzer MAVR is an operating experimental facility used with the beams of the U400 cyclotron and the DRIBs radioactive ion beam complex at the Flerov Laboratory of Nuclear Reactions, Joint Institute for Nuclear Research. A number of important results have been obtained in experiments performed with the MAVR analyzer, some of which have significantly expanded our understanding of the interaction mechanisms of complex nuclei and their characteristics.

In particular, studies of nuclear reaction mechanisms with heavy-ion beams at energies $5 \leq E \leq 12$ MeV/nucleon were carried out in works [?, ?, ?, ?]. These investigations included transfer reactions, breakup of weakly bound nuclei, elastic and inelastic scattering, as well as reactions accompanied by the emission of light charged particles. In addition to studies of nuclear reaction mechanisms, correlation measurements of nuclear reaction products were performed with the analyzer, i.e. coincidence measurements of fast charged particles with fission fragments [?].

In works [?, ?], the characteristics and structure of reactions involving light exotic nuclei near the Coulomb barrier energy region were investigated using the MAVR analyzer.

2 Main characteristics of the MAVR setup

It is expected that the above-mentioned research directions will continue to develop using the beams of the U400 and U400R accelerator complexes over a wide energy range from sub-barrier energies up to several tens of MeV per nucleon. For these studies different detector systems will be used in combination with the high-resolution magnetic analyzer MAVR.

The analyzer has a large solid angle for reaction product detection (15 msr), high momentum resolution ($\sim 10^{-4}$), and large dispersion in the focal plane (1.9 m). This spectrometer allows registration of nuclear reaction products with energies up to 30 MeV per nucleon with high charge resolution ($\sim 1/60$). The comparative characteristics of the MAVR analyzer and modern magnetic spectrometers operating worldwide are presented in Table 1.

In experiments a primary beam monochromatization system is employed. In this case the monochromator function is provided by a system of two energy-degrading magnets (M1 and M2) combined with collimators installed in the beamline.

For this purpose the degrading magnets, together with the beamline elements, are equipped with special diaphragms, high-precision magnetic field sensors (NMR probes), beam profile monitors based on multi-wire proportional chambers (MWPC), and a time-of-flight (TOF) measurement system (see Fig. 1).

The analyzer magnet (MSP-144) consists of two regions separated by a step. The pole gap in the first region is 47 mm, while in the second region it is 30 mm. The

Table 1: Main parameters of the MAVR spectrometer compared with other magnetic analyzers

Parameter	MAVR		MSP 144		VAMOS		PRISMA LNL		MAGEX LNS	
	JINR (Dubna)	JINR (Dubna)	JINR (Dubna)	JINR (Dubna)	GANIL (Caen)	GANIL (Caen)	(Legnaro)	(Legnaro)	(Catania)	(Catania)
Geometry	Qv	Qh	D1	D2	Qv	Qh	Qv	D	Qv	D
$B\rho_{\max}$, Tm	1.5		1.4		1.7		1.2		1.8	
Deflection angle, deg	110.7		110.7		45		45		55	
Solid angle, msr	15		2.3		70		80		55	
Dispersion, cm/%	2		1.5		1.8		2		3.68	
Energy resolution, $\Delta E/E$	5×10^{-4}		5×10^{-4}		5×10^{-4}		1×10^{-3}		–	
Charge resolution, $\Delta Z/Z$	1/60		1/60		1/50		1/60		–	

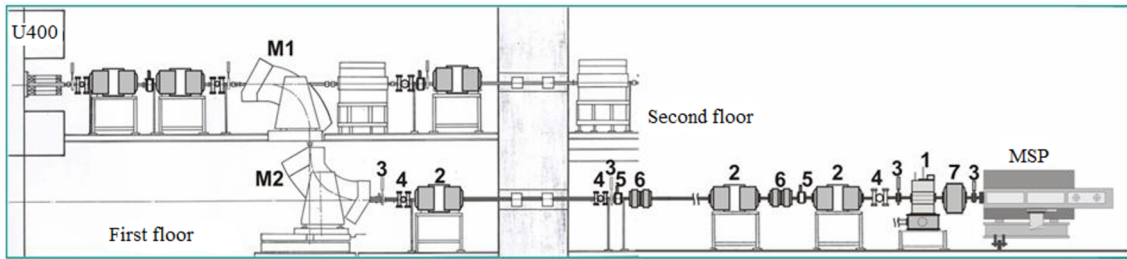


Figure 1: Layout of the MAVR analyzer on the beam channel of the cyclotron of the JINR Flerov Laboratory of Nuclear Reactions U400.

magnetic field in the first region is 1.55 times lower than in the second region.

The bending angle in the first region of the magnet is 60° , with a front edge angle of $+60^\circ$. The bending angle in the second region is 51° , with a rear edge angle of -28.5° (see Fig. 2).

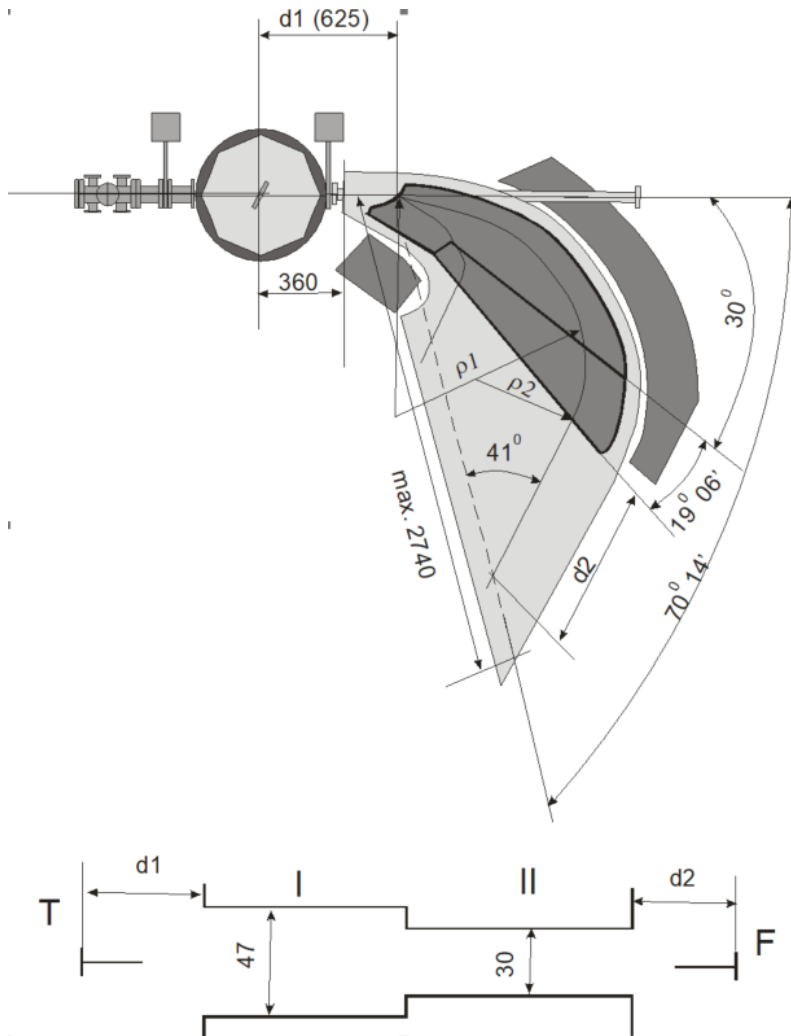


Figure 2: Schematic layout of the wide-range magnetic analyzer with stepped magnet poles MSP-144 (MAVR).

An important characteristic of the MAVR analyzer is the suppression of the primary beam relative to the reaction products. In order to calculate these param-

ters, a dedicated software package MAVRPC [?] was developed. This code allows calculation of the focal plane position of the analyzer, selection of optimal magnetic fields of the quadrupole lenses and dipole magnets, evaluation of the solid angle of the setup, as well as other optical parameters of the spectrometer.

At the initial stage of the calculations in the MAVRPC code, the following parameters are specified: the particle charge Z , the mass number A , and the energy E (in MeV) of the particle traveling through the magnetic analyzer along the central trajectory. In addition, the parameter S_0 is defined as the distance traveled by the central particle from the exit of the magnet to the focal plane, and α is the angle between the focal plane and the trajectory of the central particle after the magnet.

As an example, the MAVRPC code was used to calculate the optimal magnetic fields of the quadrupole lenses ($Q_1 = 0.33568$ T, $Q_2 = 0.35760$ T) and dipole magnets ($B_1 = 0.73$ T, $B_2 = 1.13$ T) corresponding to a focal plane position defined by the parameters $S_0 = 1$ m and $\alpha = 30^\circ$. An α particle ($Z = 2$, $A = 4$) with energy $E = 40$ MeV was chosen as the central particle. The calculated solid angle of the setup turned out to be 3.1 times larger than the solid angle of the MSP-144 analyzer (see Fig. 3).

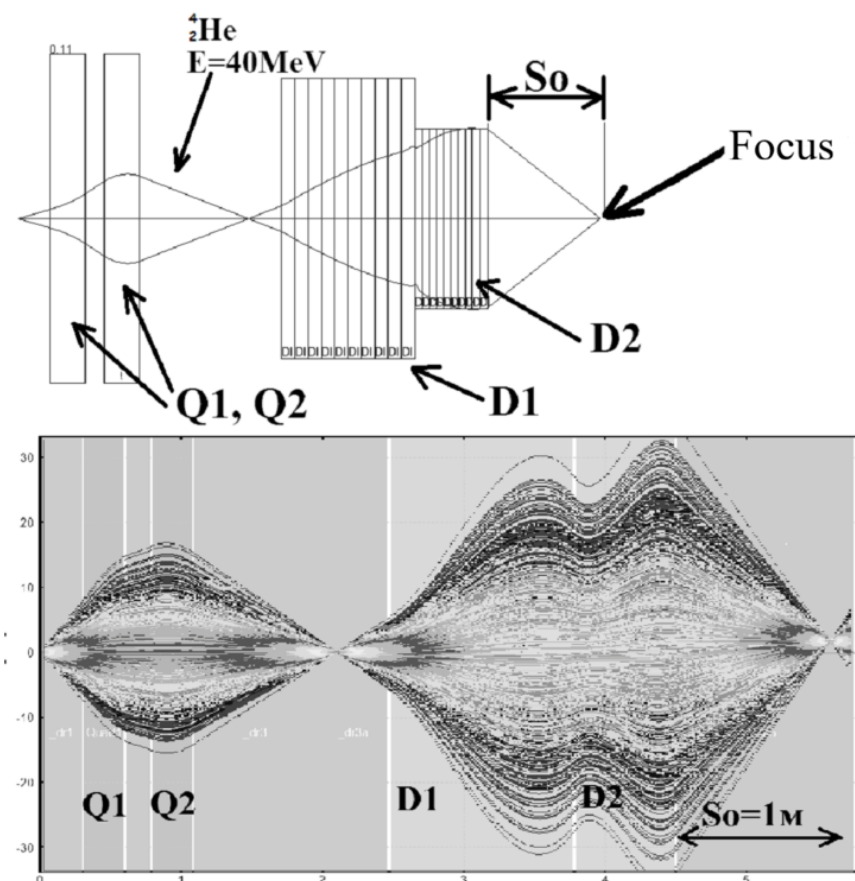


Figure 3: Trajectories of α particles with an energy of 40 MeV in the MAVR analyzer: (a) calculated using the MAVRPC software package, (b) simulated using the Monte Carlo method in the LISE++ code. Q_1 , Q_2 – quadrupole lenses; D_1 – first dipole magnet; D_2 – second dipole magnet.

After entering the corresponding input parameters, the program determines the optimal magnetic fields of the analyzer magnets and quadrupole lenses. As a

result, the magnetic fields of the first ($Q_1 = 0.33568$ T) and second quadrupole lens ($Q_2 = 0.35760$ T), as well as the fields of the first ($B_1 = 0.73$ T) and second stage of the analyzer magnet ($B_2 = 1.13$ T), are obtained. In addition, the calculated solid angle of the MAVR analyzer is determined (see Fig. 4). Specification of these parameters uniquely defines the position of the focal plane of the analyzer (see Fig. 4).

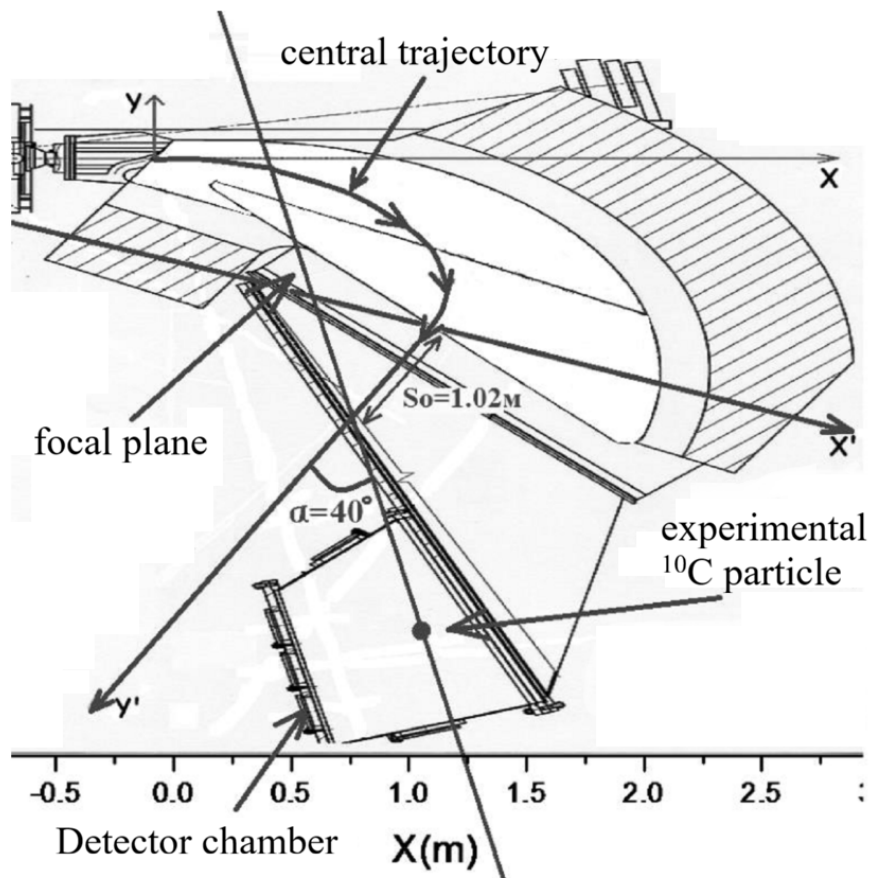


Figure 4: Graphical representation of the focal plane calculation and the position of the detected particle.

Thus, calculations of the trajectories of charged particles in the high-resolution magnetic analyzer MAVR performed using the MAVRPC software package have shown that the solid angle of the MAVR analyzer can be increased by up to a factor of three compared with the MSP-144 analyzer. At the same time the momentum resolution is $\Delta p/p \sim 1 \times 10^{-4}$, the energy resolution is $\Delta E/E \sim 5 \times 10^{-4}$, and the reaction products are detected with high charge resolution ($\Delta Z/Z \sim 1/60$).

Subsequent experimental measurements of the magnetic analyzer parameters have shown good agreement with the calculated values.

3 Detector system of the MAVR setup

A detector complex is installed in the focal plane of the MAVR analyzer, including detectors for time-of-flight measurements and a position-sensitive ionization chamber. This detector system provides high-precision measurements of the coordinates of re-

action products, allowing reconstruction of their trajectories as well as measurements of the total energy and specific energy loss of the detected particles.

For correlation experiments with the MAVR setup, a wide-aperture telescope based on silicon strip detectors is installed in the reaction chamber of the analyzer for the registration of coincident reaction products. At low incident ion energies the reactions usually have a two-body character; therefore precise registration of a reaction product in coincidence with its conjugate partner provides important information on the characteristics of the investigated process.

Reaction products and primary beam nuclei with the same momentum-to-charge ratio may be focused at the same point of the analyzer focal plane. This largely determines the separation of reaction products from the primary beam. In order to achieve a high level of suppression of the primary beam, a gas-filled mode of the analyzer chamber is used. This imposes specific requirements on the MAVR design, including thin entrance windows, separation of the vacuum system from the pumps, the use of limiting foils in front of the detector systems, and a time-of-flight detector. These solutions provide a high suppression factor, which is particularly important for heavy reaction products, especially in the mass region close to that of the primary beam nuclei.

3.1 Position-sensitive ionization chamber

The main element of the detector system installed in the focal plane of the analyzer is a position-sensitive ionization chamber (PSIC), which allows measurement of the specific ionization energy loss using a segmented anode, as well as determination of the horizontal coordinate of the particle hit position. The latter is achieved by means of a resistive wire operating in the proportional gas mode and a delay line.

For the registration of long-range particles, a mosaic of semiconductor detectors and a CsI crystal optically coupled to a photomultiplier tube is installed behind the working volume of the PSIC (not shown in Fig. 5). The position-sensitive ionization chamber (PSIC) consists of an entrance window, an anode, a cathode, and a Frisch grid.

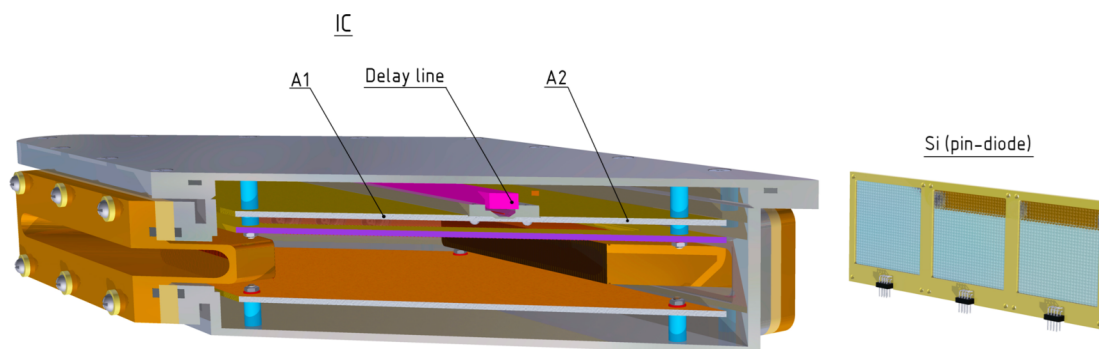


Figure 5: Schematic layout of the detector system of the MAVR magnetic analyzer.

The entrance window of the ionization chamber has dimensions 18×260 mm and is made of a Mylar foil with a thickness of $2.5 \mu\text{m}$. The foil is glued with epoxy resin and supported by a beryllium bronze grid with a wire diameter of 0.2 mm wound on a frame with a pitch of 2 mm. Tests have shown that this design of the

entrance window allows operation of the detector at pressures up to 500 Torr without degrading the vacuum in the magnetic spectrometer chamber.

The anode and cathode of the ionization chamber are made of stainless steel and mounted on the chamber body using Teflon insulators. This technical solution significantly reduces the capacitance of the electrodes relative to ground, which is important for achieving good energy resolution. The electrodes have a rhombic shape with an inclination angle equal to the incidence angle of the particles on the focal plane. The Frisch grid is made of beryllium bronze with a wire diameter of $50\ \mu\text{m}$ and a pitch of 1 mm. Pentane or hexane vapors are used as the working gas.

The anode of the PSIC is divided into two sections, A_1 and A_2 (Fig. 5). The first section is used to measure the energy loss ΔE , while the second section measures the residual energy E . A proportional detector with a delay line is placed between the two anode sections to measure the horizontal coordinate x .

The sensitive element of this detector is a wire with a diameter of $20\ \mu\text{m}$ providing gas amplification of the electrons produced by ionization of the working gas when particles pass through the chamber. A high voltage of about 1.5 kV applied to the wire leads to further multiplication of secondary electrons and formation of signals with amplitudes up to 1 V.

The coordinate x is determined from the difference in arrival times of the signals at the ends of the delay line, which is made in the form of a solenoid and located behind the proportional wire. The characteristic impedance of the delay line is $1\ \text{k}\Omega$. The time difference between the signals is converted into an amplitude using a time-to-amplitude converter. The achieved spatial resolution is $\Delta x = 1\ \text{mm}$. Taking into account the dispersion of the magnetic analyzer $\delta = 2\ \text{cm}/\%$, this spatial resolution allows the momentum of the detected particles to be measured with an accuracy of $\Delta p/p \sim 10^{-4}$.

3.2 Silicon detector mosaic

As mentioned above, a mosaic of semiconductor detectors installed at the exit of the PSIC is used for the registration of long-range particles. Silicon strip detectors with an active area of $55 \times 55\ \text{mm}^2$ and thicknesses ranging from $100\ \mu\text{m}$ to 1 mm are used for this purpose. Photographs of the detectors used are shown in Fig. 6.

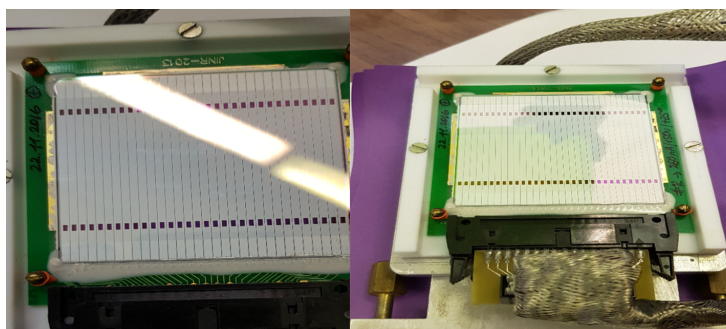


Figure 6: Photograph of double-sided silicon strip detectors with 32 strips.

Each detector surface contains 32 strips with a strip width of 1.5 mm. Such detectors can be used both for measurements of the specific energy loss ΔE and the residual energy E_r , as well as for the detection of α decay of heavy reaction products (in future studies).

The energy resolution of the silicon detectors, which have a relatively large active area and therefore a significant capacitance C , is about 40 keV. This resolution is sufficient for precise identification of the reaction products according to their mass number A and atomic number Z .

Particle identification by mass and charge was performed using measurements of the total energy ($E_{\text{tot}} = E_1 + E_r$), the energy loss ΔE , and the coordinate x of the particle hit position in the focal plane. For a clearer representation of the yields of the identified isotopes, two-dimensional matrices were constructed, as shown in Fig. 7. It can be seen that in this experimental configuration a good separation of different isotopes is achieved, allowing unambiguous identification of the reaction products and determination of their production cross sections. The performance of the chamber and its parameters were tested with extracted ion beams from the U400 cyclotron: ^{14}N (120 MeV) on a ^{12}C target. The gas pressure in the PSIC was sufficient to stop the detected ions within the volume of the ionization chamber. An argon–methane mixture (the so-called P10 mixture with 10% methane) was used as the working gas. For complete stopping of the detected products, heavier gases such as pentane (C_5H_{12}) or hexane (C_6H_{14}) vapors were also used with saturated vapor pressures of 420 and 124 Torr, respectively. The energy resolution of the ionization chamber is about 0.5 MeV.

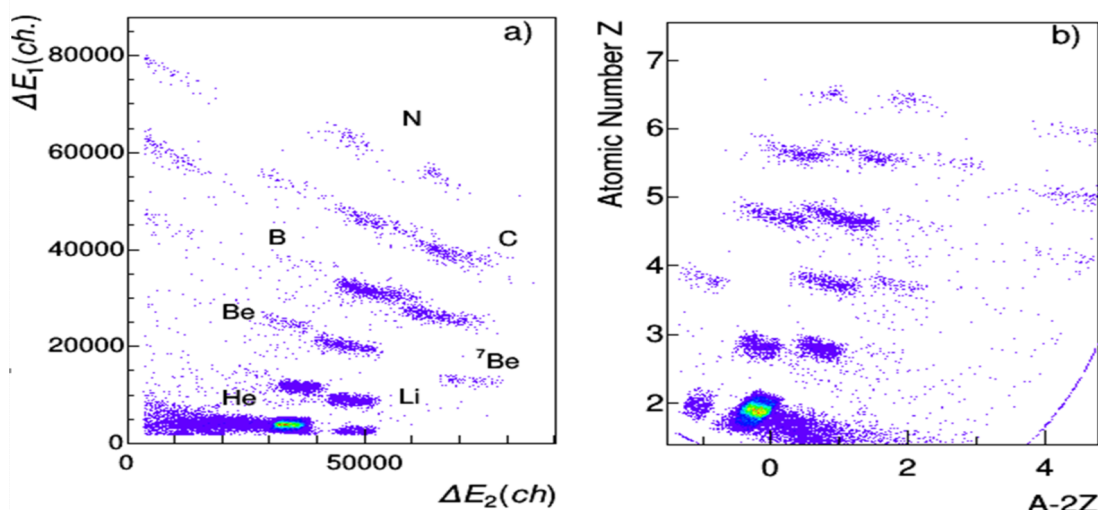


Figure 7: (a) Identification of reaction products using the $\Delta E - E_r$ method based on measurements of the specific energy loss and residual energy. (b) Identification of reaction products by mass number A and atomic number Z based on measurements of the total energy ($E_{\text{tot}} = E_1 + E_r$), specific energy loss, and the coordinate x of the particle hit position in the focal plane.

The charge distribution of the reaction products obtained in the ^{14}N (120 MeV) + ^{12}C reaction is shown in Fig. 8a. Several well-separated peaks corresponding to different atomic numbers Z are clearly observed. The peaks exhibit a narrow width with a charge resolution of about $\sigma_Z \approx 0.08$, which ensures a reliable separation of neighboring elements in the detected reaction products. Figure 8b presents the mass distribution for Be isotopes ($Z = 4$). Distinct peaks corresponding to individual isotopes are observed. The measured mass resolution is $\sigma_A \approx 0.16$ a.m.u., which allows clear identification of the isotopic composition of the reaction products.

It can be seen that the peaks are well separated from each other and the background level is relatively low. This demonstrates the good performance of the detector system and confirms that the combination of measurements of the total energy, energy loss, and particle trajectory in the spectrometer provides reliable event-by-event identification of reaction products by both atomic number Z and mass number A .

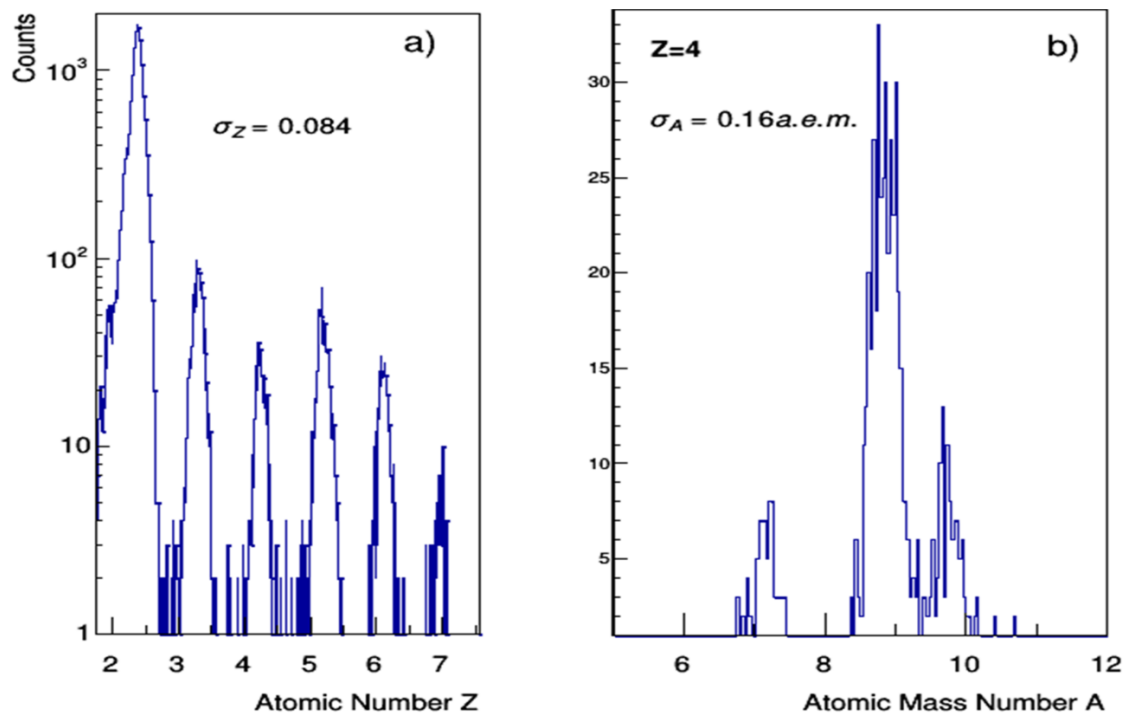


Figure 8: (a) Charge distribution of the reaction products obtained in the ^{14}N (120 MeV) + ^{12}C reaction. (b) Mass number distribution for Be isotopes.

4 Gas-filled mode of the MAVR analyzer

In order to increase the efficiency of detecting nuclear reaction products due to a narrower ionic charge-state distribution in gas, the MAVR analyzer is planned to be tested in a gas-filled mode. For heavy ions starting from carbon, charge-state distributions are observed, while lighter ions usually emerge fully stripped. The heavier the reaction products, the broader their charge-state distributions and the larger their contribution. This not only reduces the detection efficiency but also significantly complicates particle identification, since many additional spots appear in the identification matrix, making their interpretation difficult. This situation can be improved by filling the analyzer with a low-pressure gas.

Magnetic spectrometers are widely used for the detection and identification of light and heavy ions. The magnetic rigidity, defined as the ratio of the ion momentum to its electric charge, determines the trajectory of the ion in the magnetic field and remains constant along the ion path in vacuum. The dispersion of ions with different magnetic rigidities results in their spatial separation in the focal plane of the spectrometer, which can be measured with high resolution. Together with other parameters, such as energy or velocity, this allows identification of the ions.

For heavy ions the situation becomes more complicated because after passing through matter (for example a target) ions emerge with different charge states. Such ions follow different trajectories in the magnetic field depending on their charge state. On the other hand, ions with the same mass number (isobars) will have identical trajectories if they have the same energy and charge state, and therefore they cannot be separated by the spectrometer.

If the magnetic field region is filled with gas, ions undergo atomic collisions in which electrons can be captured or lost, changing the ion charge states. If the mean free path between charge-changing collisions is sufficiently small compared with the ion range in the gas, the particles follow trajectories determined by the average magnetic rigidity corresponding to the average charge state.

For ions with the same mass number but different atomic numbers Z , the average charge state in gas is different and therefore their trajectories in the magnetic field become spatially separated. Moreover, since the mean ion charge Q depends on the atomic number Z and is proportional to the ion velocity ($Q \sim vZ^{1/3}$, Bohr formula), the magnetic rigidity

$$B\rho \sim \frac{p}{Q} \sim \frac{mv}{Q} \sim \frac{m}{Z^{1/3}}$$

becomes almost independent of the ion velocity (energy). Thus the trajectories are mainly determined by the mass number A and atomic number Z , resulting in an almost velocity-independent focusing.

The problem of determining the mean charge state of heavy ions in gas has been well studied for heavy nuclei at low energies (less than 1 MeV per nucleon) [?]. However, the charge-state systematics obtained in these works are not applicable in the energy range of several MeV per nucleon, since they lead to mean charge values exceeding the atomic number Z of the nucleus, which is physically impossible.

This discrepancy is apparently related to the requirement that the magnetic rigidity $B\rho$ of heavy ions in gas remains independent of their energy. Since $B\rho \sim p/Q$, an increase in the ion energy, and therefore its momentum, requires a corresponding increase in the ion charge in order to keep $B\rho$ constant. At sufficiently high energies this leads to unrealistically large values of the mean charge.

For energies of several MeV per nucleon, the mean charge of heavy ions in gas may instead be estimated using systematics obtained for solid targets. For example, for ^{58}Ni at an energy of 350 MeV the Nikolaev-Dmitriev systematics [?] gives a mean charge $Q = 24$ at $B\rho = 0.85$, which is in good agreement with the experimental data reported in Ref. [?].

Therefore, in order to estimate the required magnetic rigidity of the spectrometer, calculations were performed using the Nikolaev–Dmitriev systematics for various heavy ions from sulfur to uranium at energies of 5 and 10 MeV per nucleon, which are typical for our experiments. The results of these calculations are presented in Table 2. These results demonstrate that the magnetic rigidity of the existing MAVR analyzer is sufficient for detecting such heavy ions in the gas-filled mode.

A dedicated gas handling system [?] was used for precise setting of the gas pressure, its variation, filling of the analyzer, regulation of the gas flow, and stabilization of the pressure inside the analyzer.

Thus, the MAVR setup represents a unique magnetic analyzer with record-high performance for several key parameters. Its capabilities have made it possible to

Table 2: Calculated mean charge states $\langle Q \rangle$ and magnetic rigidity $B\rho$ for heavy ions at energies of 5 and 10 MeV per nucleon according to the Nikolaev–Dmitriev systematics.

Isotope	A	Z	E (MeV/A)	$\langle Q \rangle$	$B\rho$ (Tm)
^{36}S	36	16	5	14.2	0.82
^{48}Ca	48	20	5	17.4	0.89
^{50}Ti	50	22	5	19.0	0.85
^{56}Fe	56	26	5	22.0	0.82
^{58}Ni	58	28	5	23.5	0.79
^{64}Zn	64	30	5	25.0	0.82
^{78}Kr	78	36	5	29.4	0.85
^{90}Zr	90	40	5	32.2	0.90
^{102}Pd	102	46	5	36.3	0.90
^{124}Sn	124	50	5	38.9	1.02
^{139}La	139	57	5	43.5	1.03
^{184}W	184	74	5	53.9	1.10
^{208}Pb	208	82	5	58.6	1.14
^{238}U	238	92	5	64.3	1.19
^{36}S	36	16	10	14.9	1.10
^{48}Ca	48	20	10	18.4	1.19
^{50}Ti	50	22	10	20.2	1.13
^{56}Fe	56	26	10	23.6	1.08
^{58}Ni	58	28	10	25.2	1.05
^{64}Zn	64	30	10	26.9	1.08
^{78}Kr	78	36	10	31.8	1.11
^{90}Zr	90	40	10	35.1	1.17
^{102}Pd	102	46	10	39.8	1.17
^{124}Sn	124	50	10	42.9	1.31
^{139}La	139	57	10	48.2	1.31
^{184}W	184	74	10	60.7	1.38
^{208}Pb	208	82	10	66.4	1.43
^{238}U	238	92	10	73.3	1.48

perform a number of experiments that have provided important and, in many cases, unexpected physical results.

5 Conclusion

The high-resolution magnetic analyzer MAVR has been developed and successfully commissioned for experiments with stable and radioactive ion beams at the U400 cyclotron and the DRIBs facility at JINR. The analyzer demonstrates high momentum resolution ($\Delta p/p \sim 10^{-4}$) and enables reliable event-by-event identification of reaction products by their mass number A and atomic number Z using a detector system based on a position-sensitive ionization chamber and silicon detectors. Experimental studies confirm high charge and mass resolution of the system. The feasibility of operating the analyzer in a gas-filled mode has been demonstrated, indicating its applicability for studies of heavy ions in the energy range of several

MeV per nucleon.

References

- [1] A. K. Azhibekov, V. A. Zernyshkin, V. A. Maslov, Yu. E. Penionzhkevich *et al.*, Phys. At. Nucl. **83**, 94 (2020) (In Russian).
- [2] R. Kalpakchieva, V. A. Maslov, R. A. Astabatian *et al.*, Phys. At. Nucl. **70**, 619 (2007).
- [3] V. A. Maslov, R. A. Astabatyan, V. A. Damaskin *et al.*, Phys. Part. Nucl. Lett. **8**, 31 (2011).
- [4] Yu. E. Penionzhkevich, V. V. Samarin, S. M. Lukyanov, V. A. Maslov, M. A. Naumenko, Chin. Phys. C **46**, 114002 (2022).
- [5] D. Aznabaev, S. M. Lukyanov, Zh. Zeinulla, T. Isataev, V. A. Maslov, K. Mendibaev, E. V. Melnik, S. S. Stukalov, V. I. Smirnov, A. V. Shakhov, Eurasian J. Phys. Funct. Mater. **5**, 88 (2021) (In Russian).
- [6] Yu. E. Penionzhkevich, R. Kalpakchieva, A. A. Kulko, S. M. Lukyanov, V. A. Maslov, N. K. Skobelev, Int. J. Mod. Phys. E **17**, 2349 (2008).
- [7] S. M. Lukyanov, A. S. Denikin, E. I. Voskoboynik, S. V. Khlebnikov, M. N. Harakeh, V. A. Maslov, Yu. E. Penionzhkevich, Yu. G. Sobolev, W. H. Trzaska, G. P. Tyurin, K. A. Kuterbekov, J. Phys. G **41**, 035102 (2014).
- [8] V. A. Maslov, V. A. Zernyshkin, Yu. E. Penionzhkevich, I. V. Kolesov, O. B. Tarasov, Eurasian J. Phys. Funct. Mater. **3**, 24 (2019).
- [9] M. Paul *et al.*, Nucl. Instrum. Methods A **277**, 418 (1989).
- [10] K. E. Gregorich *et al.*, Nucl. Instrum. Methods A **711**, 47 (2013).
- [11] V. S. Nikolaev and I. S. Dmitriev, Phys. Lett. A **28**, 277 (1968).
- [12] I. V. Butusov, V. A. Maslov, K. Mendibaev, A. V. Shakhov, JINR Preprint R3-2023-13 (2023) (In Russian).